

Deneb is a Large Amplitude Polarimetric Variable

DANIEL V. COTTON ^{1,2} JEREMY BAILEY ^{3,2} JEAN PERKINS ¹ DEREK L. BUZASI ⁴ AND IEVGENIIA BOIKO ^{1,5}

¹Monterey Institute for Research in Astronomy, 200 Eighth Street, Marina, CA 93933, USA.

²Western Sydney University, Locked Bag 1797, Penrith-South DC, NSW 2751, Australia.

³School of Physics, University of New South Wales, Sydney, NSW 2052, Australia.

⁴Department of Chemistry & Physics, Florida Gulf Coast University, 10501 FGCU Boulevard S., Fort Myers, FL 33965, USA.

⁵California State University, Long Beach, 1250 Bellflower Blvd, Long Beach, CA 90840, USA.

ABSTRACT

We write to report the discovery that Deneb is a large amplitude polarization variable. Over a ~ 400 d time span from August 2022 Deneb’s polarization was typically around 3900 parts-per-million (ppm) in the SDSS g' -band. Yet, it varied by several hundred ppm in an irregular way on a timescale of weeks. The largest polarization change, amounting to 2500 ppm, occurred shortly after the last pulsation “resumption” event identified by [Abt et al. \(2023\)](#) in *TESS* photometry. The relationship between the observed polarization – particularly corresponding to the resumption event – and its brightness and H_α spectra suggests a mechanism involving density changes in its wind and/or extended atmosphere. Smaller effects due to pulsations are not ruled out and further study is recommended.

Keywords: Alpha Cygni variable stars (2122), Starlight Polarization (1571), Polarimetry (1278)

1. INTRODUCTION

Deneb (α Cygni, HD 197345) is a type A2Ia supergiant, and the 19th brightest star in the night sky ($m_V = 1.25$). It has long been known to be variable photometrically ($\Delta m \approx 0.08$, [Fath 1935](#)) and in radial velocity (RV) ($\Delta v = 15.5$ km/s, [Paddock 1935](#)) on similar timescales. [Abt \(1957\)](#) found Deneb’s behaviour to be typical of intermediate type supergiants, and concluded radial pulsations were the most likely cause. In re-examining [Paddock’s](#) data, [Lucy \(1976\)](#) identified many periods, and attributed its stable semi-regular variability to the simultaneous excitation of many discrete non-radial pulsation modes. Though sparse, other studies have found inconsistent periods in Deneb’s RV and photometry. For example [Richardson et al. \(2011\)](#) identified transient periods of ≈ 40 d in H_α structure but 13.4 and 17.8 d in photometry and Si II RV.

Last year [Rzaev \(2023\)](#), by applying line profile analysis, concluded periods of 12-14 d and ~ 22 d to be due to radial and non-radial pulsations respectively. Even more recently [Abt et al. \(2023\)](#) identified a pattern for resumptions of the 11-12 d pulsation cycle in flux and RV, where they are triggered irregularly at multiples of 72.4 ± 0.3 d – according to [Rzaev \(2023\)](#) the events last $\approx 34 \pm 1$ d. Mode identification would enable asteroseismology, but this has proved difficult for other massive non-radial pulsators, even combining spectroscopy and photometry.

Many other early-type supergiants were added to the α Cygni variable class, of which Deneb is the proto-

type, after the precise space-based photometry of the *Hipparcos* mission revealed their variability ([Adelman & Albayrak 1997](#); [Waelkens et al. 1998](#)). The presumed mechanism, non-radial pulsations, is written into the class definition¹. However, more recent high-cadence space photometry reveals supergiant variability to be stochastic in nature with a red-noise type frequency distribution. Proposed mechanisms for which include internal gravity waves ([Bowman et al. 2019](#)), sub-surface convection regions ([Cantiello et al. 2021](#)), and instabilities in their strong radiatively-driven stellar winds ([Krtićka & Feldmeier 2021](#)).

Linear polarimetry provides spatial information, either in the form of normalized Stokes vectors q and u , or in total linear polarization, p , and position angle, θ . It can be used in asteroseismology to break degeneracies and enable mode determination ([Cotton et al. 2022b](#)). However, large polarization variability has been observed in other α Cygni stars, and explained as arising from scattering in a clumpy wind (e.g. [Hayes 1984, 1986](#), see also [Clarke 2010](#), Ch. 13.6). The two mechanisms can be distinguished by the scale and character of the variability.

The most recent linear polarization observations of Deneb are searches for line polarization producing non-detections (refs. within [Clarke & Brooks 1984](#)). Broad-

¹ See ‘ACYG’ in the General Catalogue of Variable Stars ([Samus et al. 2017](#), <http://www.sai.msu.ru/gcvs/gcvs/iii/vartype.txt>).

Date	λ_{eff} (nm)	n	p (ppm)	θ ($^{\circ}$)	Ref.
1949 11/29–12/15	440	4	5390 ± 1250	19 ± 7	1,2
1956–1958	462	6	3969 ± 100	29 ± 1	3
1958 N. Summer	372	6	4802 ± 148	31.8 ± 1.3	4
1958 N. Summer	430	7	4410 ± 100	37.7 ± 1.3	4
1958 N. Summer	516	5	4459 ± 123	40.2 ± 1.3	4
c1964	580	1	3969 ± 196	40.2 ± 1.4	5

Table 1. Historic observations of Deneb’s polarization. Values of total linear polarization, p , given in parts-per-million, are converted from polarization magnitudes. The third column indicates the number of individual observations. Regrettably, only [Hall & Mikesell \(1950\)](#) report the individual dates and measurements, but large nominal errors mean these are not illuminating. No correction has been made for co-ordinate precession of θ , which is $\approx 0.01^{\circ}/\text{yr}$. Refs: 1: [Hall & Mikesell \(1950\)](#), 2: [Hall \(1958\)](#), 3: [Behr \(1959a\)](#), 4: [Behr \(1959b\)](#), 5: [Serkowski & Chojnacki \(1969\)](#).

band observations, typically better constrained, were made from 1949 to ~ 1964 (Tbl. 1); most extensively by Alfred Behr, who observed first unfiltered ([Behr 1959a](#)) then in three passbands ([Behr 1959b](#)). The latter display a significant θ rotation with wavelength, ascribed to multiple line-of-sight dust clouds. In every case Deneb’s polarization is taken as interstellar, with no variability ever claimed.

We first observed Deneb as part of an, as yet, unpublished polarimetric survey of bright northern stars; follow-up observations showed obvious variability. This became part of the impetus for a large study of α Cygni stars as a class by teams in both hemispheres, a report of which will be given in a future publication. In light of [Abt et al.](#)’s call for more spectroscopy and photometry of Deneb, we present our current polarimetric data on the star, along with some pertinent calculations, to demonstrate the value polarimetry has for this work.

2. OBSERVATIONS

From 2022 August to 2023 October, high precision polarimetric observations of Deneb were made with the HIGH Precision Polarimetric Instrument 2 (HIPPI-2, [Bailey et al. 2020](#)) on MIRA’s 36-inch telescope at its Oliver Observing Station (OOS) ([Cotton et al. 2022a](#)), and with the Polarimeter using Imaging CMOS Sensor And Rotating Retarder (PICSARR, [Bailey et al. 2023](#)), first on the Celestron C14 at MIRA’s Weaver Student Observatory (WSO, [Babcock 2008](#)) and later on a 14-inch CDK co-mounted to the 36-inch. Most observations were 12 min in the g' band (errors: 7, 17, 17 ppm respectively, i.e. $\sim 10\text{--}30\times$ more precise than the best previous individual measurements); some shorter exposures were made in other SDSS bands with PICSARR. Data were reduced by the usual calibration and reduc-

tion procedures of each instrument, involving low/high polarization standard observations and a full bandpass model (without reddening). Multi-band observations of polarized standards are used to correct θ .

During this period, 8 spectra (SNR $\sim 150\text{--}200$) of Deneb over 6 nights were taken with a BACHES Minichelle spectrograph ($R\sim 35,000$) on the MIRA 36-inch. These were reduced with standard IRAF tools and procedures.

The *Transiting Exoplanet Survey Satellite* (TESS, [Ricker et al. 2014](#)) observed Deneb in Sectors 41, 55 and 56 at 120 s cadence. We used the Asteroseismology-Optimized Pipeline (AOP) software to align and process the photometric data ([Buzasi et al. 2016](#); [Nielsen et al. 2020](#); [Metcalf et al. 2023](#)). This essentially constructs an optimized photometric aperture one pixel at a time, minimizing the high-frequency noise in the resulting light curve, which is then iteratively detrended against centroid position and background – the result is a light curve that is consistently significantly better than the SPOC product for bright and/or saturated targets.

3. ANALYSIS AND DISCUSSION

3.1. Mean Polarization and Variability

The mean polarization of all 88 g' observations is $p = 3947.5$ ppm at a position angle $\theta = 33.07^{\circ}$, or in normalized Stokes parameters: $(q, u) = (1596.2, 3610.4)$ ppm. In Fig. 1(a) measurements from the two polarimeters agree well in recording polarization varying on a timescale of weeks. The variability is much larger than the median error of 16 ppm, with $(\sigma_q, \sigma_u) = (608.5, 318.9)$ ppm, thus $\sigma_p = (\sigma_q^2 + \sigma_u^2)^{1/2} = 687.0$ ppm. Tbl. 1 shows that such variability has been detectable since the second half of the 20th century. Indeed, taking account of wavelength dependence (see Sec. 3.5), comparison with Tbl. 1 implies similar past variability. The impression is strengthened by also considering the 18 individual H_{β} , H_{γ} and Ca II H line and adjacent continuum observations of [Hayes & Illing \(1974\)](#); [Hayes \(1975\)](#); [Clarke & McLean \(1976\)](#); [Clarke & Brooks \(1984\)](#)²; these mostly have errors ~ 300 ppm, but cover a range $p = 3670$ to 5400 ppm, and $\theta = 32.5$ to 42.2° .

Applying the methods of [Brooks et al. \(1994\)](#), both the kurtosis (2.6490) and skewness (5.5924) of q are significant at the 99% level (but insignificant in u at 0.0454 and 2.4200 respectively). This reflects the irregular nature of the variability recorded, with one deviation from the mean twice the magnitude of any others. There are no obvious periods but changes equating to hundreds of ppm are seen to occur on a timescale of weeks. Together with the sparsity of observations, this explains how Deneb’s polarimetric variability has gone unnoticed until now.

² In some of this work Deneb is used as a stable reference to check the reliability of the instrument.

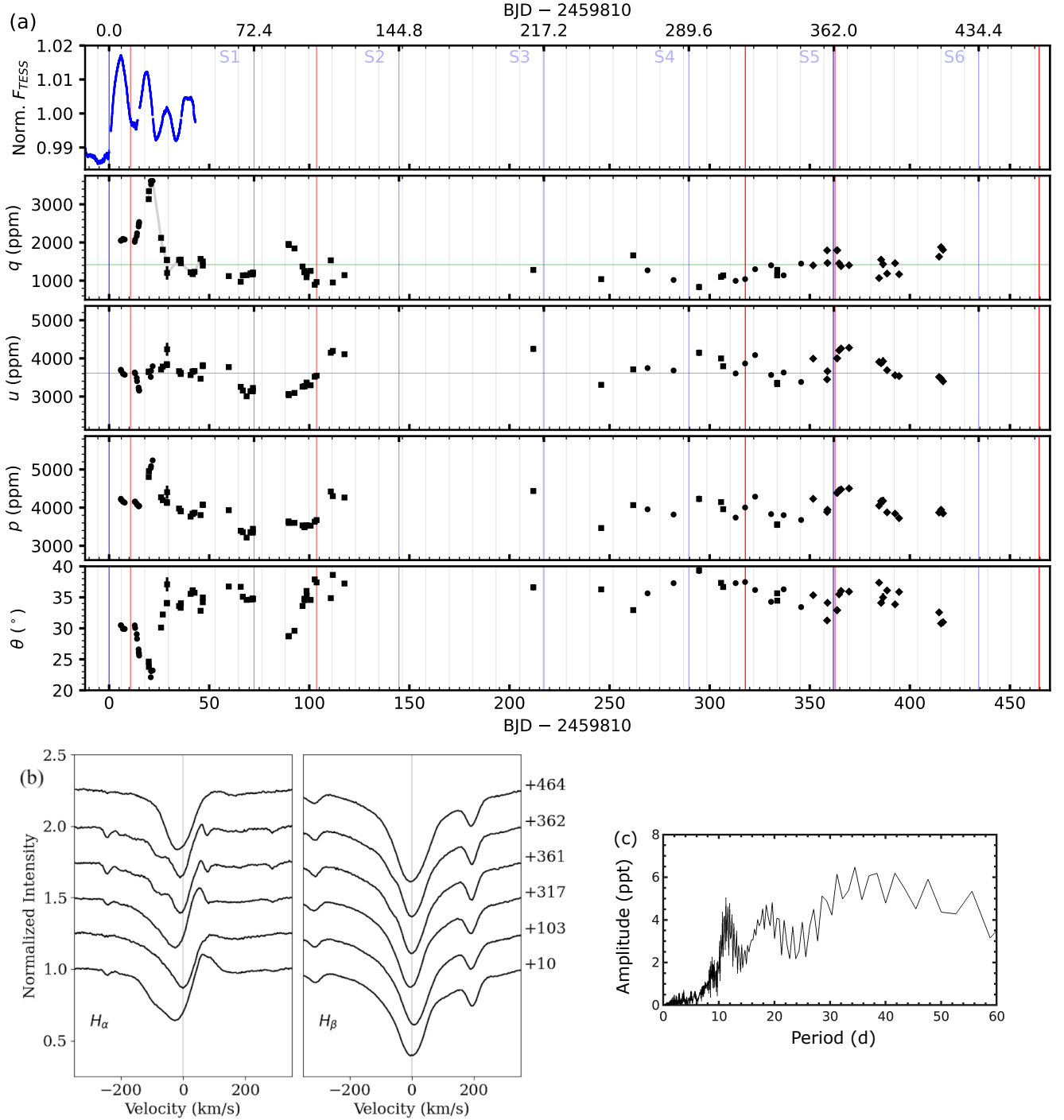


Figure 1. Observational data. (a) Time series data from Sector 55 and 56 *TESS* photometry [top panel] and g' -band polarimetry (HIPPI-2/36-inch/OOS – circles, PICSARR/C14/WSO – squares, PICSARR/CDK-14/OOS – diamonds) [bottom four panels]. The time series are divided into a number of segments, which we denote S[n]; these are all 72.4 d in length corresponding to the semi-regular cycle for the “resumption” events. The beginning of the first segment is 2459810 BJD, which is the last resumption event identified by [Abt et al. \(2023\)](#). Deneb’s 11.7 d pulsation cycle can be seen in the *TESS* data; the grey grid lines are placed every 11.7 days offset to +6.1 d to correspond with the first photometric maximum. Green lines are the medians in q (1418.5 ppm) and u (3612.5 ppm). A grey line guides the eye in q after the extreme event. The red lines correspond to the BJD dates BACHES spectra (SNR = 150-200) were taken; these are shown in (b) centred on H_α/H_β (left/right); the strongest additional absorption features are seen at +10, +361 and +362 d. (c) (Semi-) Amplitude spectrum derived from *TESS* Sectors 41, 55 and 56 in parts-per-thousand (ppt = 1000 \times ppm); prominent peaks correspond to periods of \sim 38 d, 11-12 d, and 18-20 d. Note that the frequency resolution is low due to the short length of the time series.

3.2. Candidate Polarigenic Mechanisms

Broadly speaking, for a non-magnetic (Grunhut et al. 2010), non-binary, early-type star like Deneb, intrinsic broadband linear polarization is produced by electron scattering, either at the photosphere via distortion of the stellar disc; or above it by scattering from an asymmetric gas medium. For the polarization to be variable either the symmetry or the strength of the scattering process must be changing. The two main candidates for a variable polarization are clumpy winds and non-radial stellar pulsations.

3.2.1. Polarization from Winds

Polarization variations are most easily explained as arising from scattering in a clumpy stellar wind. Hydrogen gas structures are a ubiquitous source of polarization measuring hundreds to thousands of ppm in early-type systems, such as close binaries and Be stars. Similarly large polarizations are produced in the winds of Wolf-Rayet (WR) stars, where polarimetry is used to study the wind structure (Robert et al. 1989; Moffat & Robert 1991). Polarization from this mechanism shows no preferred orientation, and though the timescale of polarimetric and photometric variability match, the signals are at best weakly correlated; the ratio of polarimetric to photometric amplitudes, σ_p/σ_F , is $\sim 1/20$.

Supergiants show polarimetric variability up to thousands of ppm (Coyne 1972). As in WR stars, in earlier type supergiants this variability is attributed to clumpy winds (Hayes 1984; Lupie & Nordsieck 1987; Bailey et al. 2024). Deneb’s polarization fluctuations are similar in scale but slower than seen in those stars. We don’t yet have enough data for a robust frequency analysis, but there is no clearly favoured polarization direction nor persistent periodicity.

Similar behaviour is seen in B8 Ia Rigel; Hayes (1986) described its polarization as aperiodic and slowly varying, with no preferred direction nor centroid. Like Deneb, Rigel exhibits semi-periodic light curve fluctuations and episodic H_α features, which Hayes took as supporting evidence for “temporally and spatially variant mass loss.” If this is the correct interpretation for both stars then we expect to see irregular photometric variability and features in H_α concordant with large polarization changes.

3.2.2. Non-radial Pulsations

Neither radial nor dipole pulsations produce polarization, but photospheric distortions caused by non-radial pulsations with mode degree $\ell \geq 2$ can produce variable polarization (Odell 1979). If this mechanism is at work, then polarimetry, photometry and RV variations will all be correlated with fixed ratios between q and u , and the other measurements. In light of the prominent RV work looking at pulsations in Deneb, we present calculations of the polarization to expect from this mechanism here.

Watson (1983)’s analytical model enables polarimetric pulsation amplitudes to be determined by multiplying the photometric amplitude by the ratio of scaling factors, $z_{\ell\lambda}/b_{\ell\lambda}$, and a term derived from the mode geometry we label $G_{\ell mi}$. The terms $b_{\ell\lambda}$ and $z_{\ell\lambda}$ are calculated from the intensity and polarization dependence on viewing angle, determined from stellar atmosphere models as described by Cotton et al. (2022b), for a given mode degree, ℓ , and wavelength, λ . $G_{\ell mi}$ – which is independent of stellar type – is a function of ℓ , azimuthal order, m , and inclination, i (see Cotton et al. 2022b Fig. 4).

In the top panels of Fig. 2 we have calculated a range of $z_{\ell\lambda}/b_{\ell\lambda}$ values for both Deneb and β Cru. In the lower panels the distribution of $G_{\ell mi}$ is shown for a representative grid of geometries. Together the product of upper and lower panels shows that polarimetric pulsation amplitudes will typically be ~ 1000 times smaller than photometric, but that in a few rare cases they might actually be larger (i.e. where $N > 0$ in the lower panel for values of $G_{\ell mi}$ exceeding the inverse of any point on the line in the corresponding upper panel).

The only polarimetric pulsation detections to date are in β Cru (Cotton et al. 2022b), which is presented for comparison in Fig. 2. Polarization semi-amplitudes of up to ≈ 10 ppm were produced in β Cru from a mode with an amplitude 30-40 \times smaller than the largest noted in Deneb, so larger effects are possible even though the most likely variability is of a similar scale. The calculations also show that multi-band observations are likely to be a useful diagnostic since the amplitudes will be different, and in some cases – where z_{ℓ}/b_{ℓ} changes sign – of opposite phase.

3.3. Photometric Frequency Analysis

We performed a straightforward frequency analysis of the *TESS* data, combining all three sectors, applying a simple linear detrending to the entire time series, and using a 4 \times oversampled DFT. The result, presented in Fig. 1(c), reveals periodicities typical of past eras. The prominent peak at 11-12 d corresponds to that first seen by Paddock (1935), others are seen at 18-20 d and ~ 38 d. Though time series length makes the latter less significant, it is consistent with the ≈ 40 d period identified in H_α by Richardson et al. (2011), half the $n \times 72.4$ d resumption intervals described by Abt et al. (2023), and double the 18-20 d peak (also about that seen by Lucy 1976; Rzaev 2023). If there was a large polarization signal from non-radial pulsations we would expect it to manifest at one of these three detected periods, but none is obvious.

The distinct periods are embedded on a red noise background (i.e. increasing power to longer periods). This is significant since it represents stochastic variability, which could be the counter-part photometric signal to polarization induced by clumpy winds. The photometric to polarimetric amplitude ratio, $\sigma_p/\sigma_F \sim 1/11$ is larger but of the same order as that seen in WR stars.

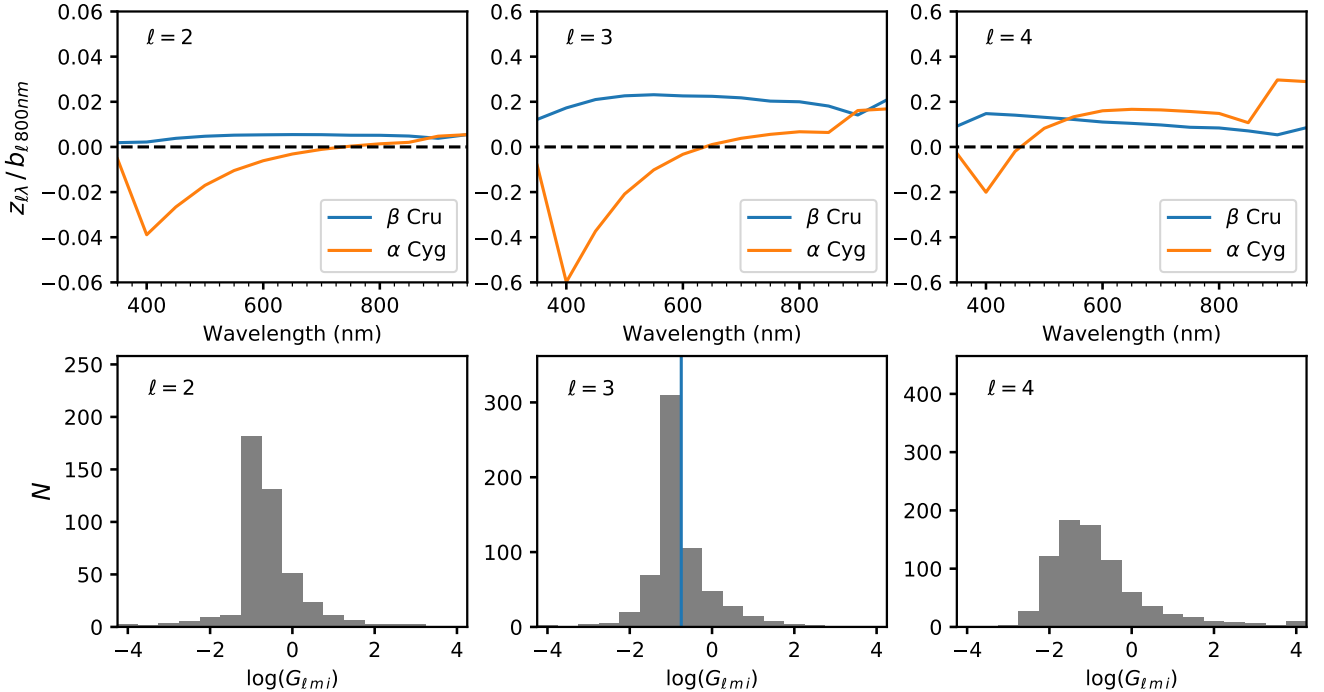


Figure 2. Following [Watson \(1983\)](#)’s analytical model, the ratio of the polarimetric to photometric pulsation amplitudes is equal to $z_{\ell}/b_{\ell} \times G_{\ell m i}$. In the upper panels is the ratio of the photometric scaling factor, b_{ℓ} , at 800 nm ($\sim TESS \lambda_{\text{eff}}$) and the polarimetric scaling factor, $z_{\ell\lambda}$ for mode degree, $\ell = 2$ (left), 3 (centre) and 4 (right) for both Deneb ($T_{\text{eff}} = 8500$ K and $\log g = 1.100$ dex) and β Cru. In the lower panels are histograms showing the distribution of values of the geometric factor, $G_{\ell m i}$, in which q and u amplitudes are combined as the root sum of the squares. One model instance, N , is calculated for each inclination, i , between 1° and 89° in one degree increments, and each $m = -\ell, \dots, 0, \dots, +\ell$ for $\ell = 2$ (left), 3 (centre) and 4 (right). The vertical blue line indicates $G_{3,-3,46^{\circ}}$ – corresponding to the largest polarimetric amplitude detected for β Cru.

3.4. Alignment with Photometric and Spectroscopic Variability

In Fig. 1(a) the time series data is divided into segments, labelled ‘S[n]’ corresponding to the 72.4 d resumption event period; zero marks the last such event identified by [Abt et al. \(2023\)](#) at 2459810 BJD. There is no polarimetric data before this, our observations begin 5 d later. About a week after that q begins trending upward reaching its most extreme value of ≈ 3600 ppm at the next photometric minimum, whereupon the timing of local maxima in q are correlated with subsequent photometric minima. The polarimetric amplitude is attenuated much more strongly after the initial outburst than is the photometric signal³, such that by +50 d no correlation with an 11-12 d cycle is evident.

The large polarization event cannot have been produced by non-radial pulsations since in that case the photometric to polarimetric amplitude ratio would be constant. However, the two signals seem at least partly related, which suggests that radial (or dipole) pulsations may not be directly responsible for the 11-12 d photometric signal either. The H_{α} line profile at +10 d dis-

plays clear additional blue (and possibly red) shifted absorption in the wings of the P-Cygni profile (Fig. 1(b)); a likely explanation is the ejection of a large gas clump. In subsequent spectra, similar absorption features (in H_{α} and/or H_{β}) are only present at +361 and +362 d (at the S5/S6 boundary) where the polarization also deviates strongly from the median. In this case the features are stronger – both blue and red shifted – perhaps indicative of closer proximity to a smaller event. If both events do correspond to ejections then they propagate in different directions.

No polarization changes as extreme as that in S1 are seen subsequently⁴, and we have no more photometric data with which to compare. There is insufficient polarimetric data for a meaningful frequency analysis. However, smaller scale changes are noticeable on timescales of ~ 10 -40 d; some are coincident with the segment transitions: Near the S1/S2 transition p is a minimum; at the S4/S5 transition q is a minimum; at the beginning of S6 u begins to decrease. These events are perhaps easiest to identify in θ and seem to correspond to inflection points rather than abrupt changes. The pattern is

³ It is also noteworthy that the photometric signal persists beyond the 34 ± 1 d duration found in RV by [Rzaev \(2023\)](#).

⁴ The peak of the extreme event is, however, consistent with the observations of [Hall & Mikesell \(1950\)](#) in both p and θ .

Fil.	λ_{eff} (nm)	Date range JD-2459810	n	Δq (ppm)	Δu (ppm)	$\sigma_{\Delta q}$ (ppm)	$\sigma_{\Delta u}$ (ppm)	$\bar{\text{Err.}}$ (ppm)	\bar{p}_{imp} (ppm)	$\bar{\theta}_{\text{imp}}$ ($^{\circ}$)
u'	377	33 – 98	11	+300.1	-164.3	53.5	113.1	55.9	3852.7	31.75
g'	468	5 – 416	88						3881.0	34.28
r'	614	33 – 66	10	-221.2	-143.7	66.2	90.7	27.1	3669.5	35.48
i'	762	66 – 98	2	-250.3	-515.9	52.2	19.1	31.0	3309.6	34.66
z'	892	68 – 117	18	-551.9	-1119.9	98.6	63.5	48.4	2639.0	35.41

Table 2. Multi-band polarimetry summary. Columns 3-9 correspond to observations concurrent with g' to which the difference is taken; 10-11 are calculated by first adding the median g' q and u values to Δq and Δu for each other band.

somewhat subjective, but if it persists it might be indicative of a deeper process that propagates through to the photosphere and drives the winds. Such a hypothesis would be best tested with simultaneous spectroscopic (incl. RV) and polarimetric data with nightly cadence. The line cores of H_{α} and H_{β} shift relative to lines more representative of the photosphere in Fig. 1(b), however our spectroscopic data is not extensive enough, as yet, to search for meaningful periodicities or connections.

3.5. Wavelength Dependence

On 28 occasions observations were made in one or more other SDSS bands alongside g' with PICSARR (within 35 mins). In Tbl. 2 we summarize these in terms of the difference $\Delta[q/u] = [q/u]_{fil} - [q/u]_{g'}$ in order to examine wavelength dependence independent of the dominant trends in polarization. To first order the multi-band observations are offset from but otherwise follow the same trends as those evident in g' – i.e. the standard deviations in Δq and Δu are mostly 1-2 σ . Only for $r' - g'$ is $\sigma_{\Delta u} > 3\sigma$. However, the nominal errors for the u' and z' bands are larger, so those measurements are not as sensitive (partly due to the camera quantum efficiency curve, but also because of shorter non- g' exposures, so future improvement will not be difficult).

Whether the variable component of the polarization is wavelength independent or not is important, since this will discriminate between optically thin wind structures (independent) and either optically thick ones or another mechanism (dependent). Non-radial pulsations could be such a mechanism. Dual filter observations such as these will account for an optically thin wind if it is insubstantial enough to see through to the photosphere. The scale of variability reflected in Tbl. 2 is consistent with what we could expect in this case from the pulsation calculations in Sec. 3.2.2; any differential pulsation signal is constrained to be $\lesssim 100$ ppm. So far the multi-band data does not reflect the expected difference in sign (i.e. phase), but it is too sparse to draw conclusions yet.

In Tbl. 2 p and θ are the values implied by adding the median g' q and u values to the mean band differences. A 3-parameter Serkowski Law (1968) fit to the individual data points modified in the same way (incl. 29 common g' points) gives the maximum interstellar polarization $p_{\text{max}} = 3898 \pm 9$ ppm, at a wavelength $\lambda_{\text{max}} = 464 \pm 6$ nm, with “constant” $K = 0.87 \pm 0.04$. The exact value of λ_{max} is sensitive to the assumed (median) g' value, but regardless is bluer than the typical

Galactic value of 550 nm (Serkowski et al. 1975), which implies smaller grains and/or another component.

The Serkowski fit reduced χ^2 is only 4.35: p is high in u' and low in z' . Assuming the adopted (median) g' values are truly representative – and if, as Hayes (1986) reports for Rigel, there is no clear centroid, it might not be – together with the complex $\theta(\lambda)$ behaviour, this indicates multiple constant polarization components. Behr (1959b)’s explanation – two or more distinct dust clouds on Deneb’s sight line – seems likely given the star’s proximity on the sky to the Pelican nebula, but other contributions, such as from an asymmetric wind (as suggested by interferometry, Chesneau et al. 2010), are not ruled out. Coyne (1972) thought similar behaviour in $p(\lambda)$ observed for other supergiants was intrinsic in origin.

4. CONCLUSIONS

Extraordinarily, the broadband polarization observations of Deneb reported here are the first such measurements in about 60 years. They reveal conclusively for the first time that the star is a large amplitude polarization variable. The median polarization in g' is $p = 3881.0$ ppm and $\sigma_p = 687.0$ ppm, about 1/11th of the flux variability.

An event producing large polarization occurred shortly after the last pulsation resumption event identified by Abt et al. (2023) in *TESS* photometry. Deneb’s dominant polarization signature appears related to its photometric variations in a way that probably indicates structures in its winds or extended atmosphere, which would make asteroseismology difficult. However, the presence of a smaller signal due to pulsation is not ruled out; future multi-band polarimetric observations will provide an invaluable diagnostic in this respect. We plan such observations concurrent with spectroscopy to correspond with upcoming *TESS* photometry. Abt et al. (2023) called for more photometry and spectroscopy of Deneb; polarimetry is also critical to understanding this enigmatic object.

We thank the Friends of MIRA for their support, Normandy Filcek for observing assistance, Sarbani Basu for help acquiring a reference, and Wm. Bruce Weaver for bringing our attention to Abt et al. (2023) as well as useful comments on the manuscript.

Data Statement: The raw *TESS* data used in this paper can be found at DOI: 10.17909/w1wk-mn94

REFERENCES

- Abt, H. A. 1957, *ApJ*, 126, 138, doi: [10.1086/146379](https://doi.org/10.1086/146379)
- Abt, H. A., Guzik, J. A., & Jackiewicz, J. 2023, *PASP*, 135, 124201, doi: [10.1088/1538-3873/ad1118](https://doi.org/10.1088/1538-3873/ad1118)
- Adelman, S. J., & Albayrak, B. 1997, *Information Bulletin on Variable Stars*, 4541, 1
- Babcock, A. 2008, *MIRA Newsletter*, 31 (2), 4
- Bailey, J., Cotton, D. V., De Horta, A., Kedziora-Chudczer, L., & Shastri, O. 2023, *MNRAS*, 520, 1938, doi: [10.1093/mnras/stad271](https://doi.org/10.1093/mnras/stad271)
- Bailey, J., Cotton, D. V., Kedziora-Chudczer, L., De Horta, A., & Maybour, D. 2020, *PASA*, 37, e004, doi: [10.1017/pasa.2019.45](https://doi.org/10.1017/pasa.2019.45)
- Bailey, J., Howarth, I. D., Cotton, D. V., et al. 2024, *MNRAS*, 529, 374, doi: [10.1093/mnras/stae548](https://doi.org/10.1093/mnras/stae548)
- Behr, A. 1959a, *Veroeffentlichungen der Universitaets-Sternwarte zu Goettingen*, 7, 199
- . 1959b, *ZA*, 47, 54
- Bowman, D. M., Bursens, S., Pedersen, M. G., et al. 2019, *Nature Astronomy*, 3, 760, doi: [10.1038/s41550-019-0768-1](https://doi.org/10.1038/s41550-019-0768-1)
- Brooks, A., Clarke, D., & McGale, P. A. 1994, *Vistas in Astronomy*, 38, 377, doi: [10.1016/0083-6656\(94\)90011-6](https://doi.org/10.1016/0083-6656(94)90011-6)
- Buzasi, D. L., Carboneau, L., Lezcano, A., & Vydra, E. 2016, in *American Astronomical Society Meeting Abstracts*, Vol. 227, American Astronomical Society Meeting Abstracts #227, 137.06
- Cantiello, M., Lecoanet, D., Jermyn, A. S., & Grassitelli, L. 2021, *ApJ*, 915, 112, doi: [10.3847/1538-4357/ac03b0](https://doi.org/10.3847/1538-4357/ac03b0)
- Chesneau, O., Dessart, L., Mourard, D., et al. 2010, *A&A*, 521, A5, doi: [10.1051/0004-6361/201014509](https://doi.org/10.1051/0004-6361/201014509)
- Clarke, D. 2010, *Stellar Polarimetry* (Wiley-VCH Verlag GmbH & Co. KGaA, Weinheim.)
- Clarke, D., & Brooks, A. 1984, *MNRAS*, 211, 737, doi: [10.1093/mnras/211.4.737](https://doi.org/10.1093/mnras/211.4.737)
- Clarke, D., & McLean, I. S. 1976, *MNRAS*, 174, 335, doi: [10.1093/mnras/174.2.335](https://doi.org/10.1093/mnras/174.2.335)
- Cotton, D. V., Bailey, J., Larson, J., et al. 2022a, *RNAAS*, 6, 209, doi: [10.3847/2515-5172/ac996d](https://doi.org/10.3847/2515-5172/ac996d)
- Cotton, D. V., Buzasi, D. L., Aerts, C., et al. 2022b, *Nature Astronomy*, 6, 154, doi: [10.1038/s41550-021-01531-9](https://doi.org/10.1038/s41550-021-01531-9)
- Coyne, G. V. 1972, in *Colloquium on Supergiant Stars*, ed. M. Hack, Third Colloquium on Astrophysics held in Trieste, 93–107
- Fath, E. A. 1935, *Lick Observatory Bulletin*, 474, 115, doi: [10.5479/ADS/bib/1935LicOB.17.115F](https://doi.org/10.5479/ADS/bib/1935LicOB.17.115F)
- Grunhut, J. H., Wade, G. A., Hanes, D. A., & Alecian, E. 2010, *MNRAS*, 408, 2290, doi: [10.1111/j.1365-2966.2010.17275.x](https://doi.org/10.1111/j.1365-2966.2010.17275.x)
- Hall, J. S. 1958, *Publications of the U.S. Naval Observatory Second Series*, 17, 275
- Hall, J. S., & Mikesell, A. H. 1950, *Publications of the U.S. Naval Observatory Second Series*, 17, 3
- Hayes, D. P. 1975, *PASP*, 87, 609, doi: [10.1086/129820](https://doi.org/10.1086/129820)
- . 1984, *AJ*, 89, 1219, doi: [10.1086/113616](https://doi.org/10.1086/113616)
- . 1986, *ApJ*, 302, 403, doi: [10.1086/163998](https://doi.org/10.1086/163998)
- Hayes, D. P., & Illing, R. M. E. 1974, *AJ*, 79, 1430, doi: [10.1086/111696](https://doi.org/10.1086/111696)
- Krtićka, J., & Feldmeier, A. 2021, *A&A*, 648, A79, doi: [10.1051/0004-6361/202040148](https://doi.org/10.1051/0004-6361/202040148)
- Lucy, L. B. 1976, *ApJ*, 206, 499, doi: [10.1086/154405](https://doi.org/10.1086/154405)
- Lupie, O. L., & Nordsieck, K. H. 1987, *AJ*, 93, 214, doi: [10.1086/114302](https://doi.org/10.1086/114302)
- Metcalfe, T. S., Buzasi, D., Huber, D., et al. 2023, *AJ*, 166, 167, doi: [10.3847/1538-3881/ac11f7](https://doi.org/10.3847/1538-3881/ac11f7)
- Moffat, A. F. J., & Robert, C. 1991, in *Wolf-Rayet Stars and Interrelations with Other Massive Stars in Galaxies*, ed. K. A. van der Hucht & B. Hidayat, Vol. 143, 109
- Nielsen, M. B., Ball, W. H., Standing, M. R., et al. 2020, *A&A*, 641, A25, doi: [10.1051/0004-6361/202037461](https://doi.org/10.1051/0004-6361/202037461)
- Odell, A. P. 1979, *PASP*, 91, 326, doi: [10.1086/130492](https://doi.org/10.1086/130492)
- Paddock, G. F. 1935, *Lick Observatory Bulletin*, 472, 99, doi: [10.5479/ADS/bib/1935LicOB.17.99P](https://doi.org/10.5479/ADS/bib/1935LicOB.17.99P)
- Richardson, N. D., Morrison, N. D., Kryukova, E. E., & Adelman, S. J. 2011, *AJ*, 141, 17, doi: [10.1088/0004-6256/141/1/17](https://doi.org/10.1088/0004-6256/141/1/17)
- Ricker, G. R., Winn, J. N., Vanderspek, R., et al. 2014, in *Society of Photo-Optical Instrumentation Engineers (SPIE) Conference Series*, Vol. 9143, *Space Telescopes and Instrumentation 2014: Optical, Infrared, and Millimeter Wave*, ed. J. Oschmann, Jacobus M., M. Clampin, G. G. Fazio, & H. A. MacEwen, 914320, doi: [10.1117/12.2063489](https://doi.org/10.1117/12.2063489)
- Robert, C., Moffat, A. F. J., Bastien, P., Drissen, L., & St.-Louis, N. 1989, *ApJ*, 347, 1034, doi: [10.1086/168194](https://doi.org/10.1086/168194)
- Rzaev, A. K. 2023, *MNRAS*, 524, 1735, doi: [10.1093/mnras/stad1995](https://doi.org/10.1093/mnras/stad1995)
- Samus', N. N., Kazarovets, E. V., Durlevich, O. V., Kireeva, N. N., & Pastukhova, E. N. 2017, *Astronomy Reports*, 61, 80, doi: [10.1134/S1063772917010085](https://doi.org/10.1134/S1063772917010085)
- Serkowski, K. 1968, *ApJ*, 154, 115, doi: [10.1086/149744](https://doi.org/10.1086/149744)
- Serkowski, K., & Chojnacki, W. 1969, *A&A*, 1, 442
- Serkowski, K., Mathewson, D. S., & Ford, V. L. 1975, *ApJ*, 196, 261, doi: [10.1086/153410](https://doi.org/10.1086/153410)
- Waelkens, C., Aerts, C., Kestens, E., Grenon, M., & Eyser, L. 1998, *A&A*, 330, 215
- Watson, R. D. 1983, *Ap&SS*, 92, 293, doi: [10.1007/BF00651294](https://doi.org/10.1007/BF00651294)